



Journal of applied research and technology

ISSN: 1665-6423

Universidad Nacional Autónoma de México, Instituto de Ciencias Aplicadas y Tecnología

Lardizábal-G., D.; Estrada-Guel, I.; Montes, J. A.; Ramirez-Balderrama, K. A.; Soto-Figueroa, C.; Ruiz Santos, R.
Synthesis and characterization of low-cost glass-ceramic foams
for insulating applications using glass and pumice wastes
Journal of applied research and technology, vol. 18, no. 2, 2020, pp. 44-50
Universidad Nacional Autónoma de México, Instituto de Ciencias Aplicadas y Tecnología

DOI: <https://doi.org/10.14482/INDES.30.1.303.661>

Available in: <https://www.redalyc.org/articulo.oa?id=47471662001>

- How to cite
- Complete issue
- More information about this article
- Journal's webpage in redalyc.org

UNAM redalyc.org

Scientific Information System Redalyc

Network of Scientific Journals from Latin America and the Caribbean, Spain and Portugal

Project academic non-profit, developed under the open access initiative



Synthesis and characterization of low-cost glass-ceramic foams for insulating applications using glass and pumice wastes

D. Lardizábal-G.^{a,b} • I. Estrada-Guel^b • J. A. Montes^a • K. A. Ramirez-Balderrama^b •
C. Soto-Figueroa^a • R. Ruiz Santos^{a*}

^aFacultad de Ciencias Químicas, Universidad Autónoma de Chihuahua, Circuito Universitario s/n,
Campus Universitario No. 2. Chihuahua, Chihuahua, Mexico. C.P. 31136

^bCentro de Investigación en Materiales Avanzados SC (CIMAV), Av. Miguel de Cervantes 120.
Complejo Industrial Chihuahua. Chihuahua, Chihuahua, Mexico. C.P. 31136

Received 09 20 2019; accepted 01 24 2020
Available online 04 30 2020

Abstract: At present, there is an increasing need to integrate ceramic materials with insulating properties for housing construction (for energy saving), mainly in areas where extreme temperature occurs. The objective of this work was to synthesize low-cost glass-ceramic foams, using recycled glass and waste materials near to Chihuahua city, Mexico, such as pumice and limestone mineral residues; the last one was used as a foaming material. The precursors were grounded, pressed forming pellets by cold pressing, and subsequently sintered using different conditions of temperature and time. The thermal conductivity, compressive strength, bulk density, actual density and percent expansion of prepared samples were evaluated and discussed in this work. Based on the experimentation, we found that optimum sintering time for this material is 20 minutes. Following this cheap and convenient procedure, a sample obtained at 800°C showed the best properties with a density of 0.44 g/cm³ and a thermal conductivity coefficient of 0.096 W/m K. These values indicated that is feasible to synthesize these foams construction industry applications working as appropriate thermal insulators.

Keywords: Ceramic foams, residues, glass, pumice, limestone, thermal insulator

*Corresponding author.

E-mail address: rruizs@uach.mx (R. Ruiz Santos).

Peer Review under the responsibility of Universidad Nacional Autónoma de México.

1. Introduction

Ceramic foams are considered as low density and porous materials with high thermal and acoustic insulating properties. These characteristics make them very interesting for use in the construction industry (Liu et al., 2016; Presas, 2008) since thermal insulating is economically highly appreciated (Bai, Yang, Xu, Jing, & Yang, 2014). Today, there are high costs implicated to keep homes and workplaces climatized (Ji, Zhang, He, Liu, & Wang, 2015), especially in geographical areas where extreme weather predominates (Kato, Ohashi, Fuji, & Takahashi, 2008). In the north part of Mexico, construction is based on bricks made of baked clay and concrete blocks. These materials are poorly insulating. Thus, the application of polymeric coatings to compensate for this lack is frequent (Meir & Roaf, 2006). The most used polymeric insulators are expanded polyurethane or polyethylene sheets; these are typically placed outdoors because of their excellent insulating properties (their thermal conductivity coefficients; k are below 0.05 W/m K) (Ozel, 2011). However, they have the disadvantage of being highly flammable and can release toxic gases when they are in contact with heat sources; thus, these are not considered for indoor installation (Vancea & Lazău 2014). Another issue is that polymeric coatings are damaged by ultraviolet light, so a layer of protective paint must be applied to prevent its exposure, its application being recurrent at least every 5 to 8 years, increasing its maintenance costs (Sousa, Amorim, Medeiros, Mélo, & Rabello, 2006).

On the other hand, ceramic coatings such as vitrocement foams have the advantage of being able to apply both indoors and outdoors, since they are not flammable and do not release any gas. They have a higher hardness and mechanical resistance compared to polymeric counterparts (Bernardo, Cedro, Florean, & Hreglich, 2007; Ding, Ning, Wang, Shi, & Luo, 2015). The present work deals with the preparation of a low-cost ceramic glass foam, taking advantage of the high availability of local residual materials such as pumice waste (which did not meet industry requirements), being a cheap alternative with an appropriate density of 1.3 g/cm³ and natural limestone, both components have exploitation sites located only a few kilometers from Chihuahua City, Mexico. Another component is glass; it was obtained as local waste in the form of used bottles and glass containers. Limestone was used as a foaming agent, varying the content of pumice and glass waste. The samples were sintered at four temperatures 700, 750, 800 and 850°C. The raw materials were characterized by XRD; meanwhile, the synthesized samples were measured for thermal conductivity, density, porosity and compressive strength in order to determine the formulation with increased insulating properties and better mechanical performance.

2. Experimental

Each of the raw materials was grounded in a Bico pulverizer model UA until the powders reached a particle size lower than 80 mesh (177 μ m). Some mixtures were weighed, and homogeneously mixed following the proportions showed in Table 1.

Table 1. Formulation nomenclature and composition (in wt. %).

Component	Limestone	Pumice	Glass
M 5-05-90	5	5	90
M 5-10-85	5	10	85
M 5-15-80	5	15	80

Each formulation was compressed at 140 psi, generating cold-compacted samples in the form of wafers (2 x 0.5 cm). The green samples were pre-heated at 450°C for 5 minutes (using a heating ramp of 15 °C/min) in a Thermolyne 21100 tubular oven to remove residual water and prevent ruptures generated during sintering at 700, 750, 800 and 850°C. Heating was performed in an air atmosphere using a flow of 200 cm³/min. Three repetitions were made for each sintering temperature. To evaluate the effect of sintering time on the material characteristics, the 800°C sample was kept in the furnace during different times (10, 20, 30 and 40 minutes). The used methodology was in accordance with the studies of Guo et al. (2014), their study also used CaCO₃ as a foaming agent.

2.1 Measurements and characterization

The phases and crystalline characteristics of raw materials were studied by X-ray Diffraction (XRD) using a Panalytical X'Pert-Pro diffractometer model MPD working at 40 kV and 35 mA using a Cu- K α radiation with a wavelength of 0.154056 nm, collected from 5 to 80° 2 θ with a step size of 0.2°/s. The percentage of porosity was determined through optical microscopy using a Dino-lite Pro microscope. The images were analyzed with Handhel Digital software, using a statistical method to determine the average pore size. The thermal conductivity was measured with an equipment Unitherm model 2022. Density determination in powders was carried out in a Quantacrome model 1000 ultra pycnometer, using high purity nitrogen (99.999%) as testing fluid. For thermogravimetric analysis, a TGA-DSC from TA instruments

model Q600 was used, using a heating ramp of 10°C/min from room temperature to 900°C in air atmosphere. The particle morphology and elementary composition of samples was characterized through a field emission scanning electron (FEG SEM) microscope model JMS7000F; the micrographs were acquired using a low voltage (5 kV); thus, it was not necessary to cover the sample with a gold conductor coating. The expansion percentage measurements were carried out, measuring the average height of samples. The thermal conductivity test is performed on a Unitherm model 2022 equipment, based on the standard ASTM E1530 (Standard Test Method for Evaluating the Resistance to Thermal Transmission of Materials by the Guarded Heat Flow Meter Technique). The apparent density was obtained taking in account the mass-volume ratio and the total porosity (P), it was calculated from the apparent density (PB) and the actual density (P0) using the equation (Chen, Lu, & Qu, 2013):

$$P = 1 - (PB/P0) \cdot 100$$

3. Results

Raw materials were characterized through XRD to identify the present phases. Fig. 1 shows that limestone mainly contains calcium carbonate in the form of a calcite phase. The diffraction pattern confirmed its presence when it was compared with an ICDD reference PDF 00-005-0586, presenting the principal peak (104) at 29.44°. The sample also contains calcium carbonate in the form of aragonite and quartz (SiO₂) as an impurity. The pumice sample presented an amorphous diffraction pattern because this mineral is a volcanic glass (Correcher, Gomez-Ros, Dogan, García-Guinea, & Topaksu, 2017). The source of the used glass was obtained from a waste of amber glass bottles.

By itself, an amorphous material was not analyzed by XRD. Its chemical composition was determined, shown in Table 2.

Table 2. Elemental analysis of waste glass.

Element	O	Si	Ca	Na	C	Al	Mg	K
(Wt %)	40.8	33.5	9.5	8.0	5.2	1.6	1.0	0.4

XRD and TGA studies (Fig. 2) confirmed that limestone mostly contains CaCO₃ being a pore-forming compound, which during its decomposition, releases significant quantities of carbon dioxide gas. The amount of this mineral in the present formulations will remain fixed at 5% based on previous experiences and studies conducted by Wu, Boccaccini, Lee, Kershaw, and Rawlings (2006) and other authors. These studies demonstrated that this concentration reached the optimal expansion for glass-based ceramic foams (Guo et al., 2014). Pumice waste was chosen as aggregate because of its low density (1.3 g/cm³), low cost and high availability in the region. The primary pumice purpose is to serve as structural support during the synthesis of ceramic foam since when the glass reaches its softening temperature; it begins to flow. Thus, pumice contributes to preserving the shape of the piece (Bento et al., 2013). On the other hand, when the decomposition of CaCO₃ begins, it must allow the formation of pores. Pumice has a double role: keeping a balance between the expansion and structural integrity of the sample. The expansion values in Table 3 indicated that the formulation with 5% pumice waste had a better performance reaching the highest numerical value.

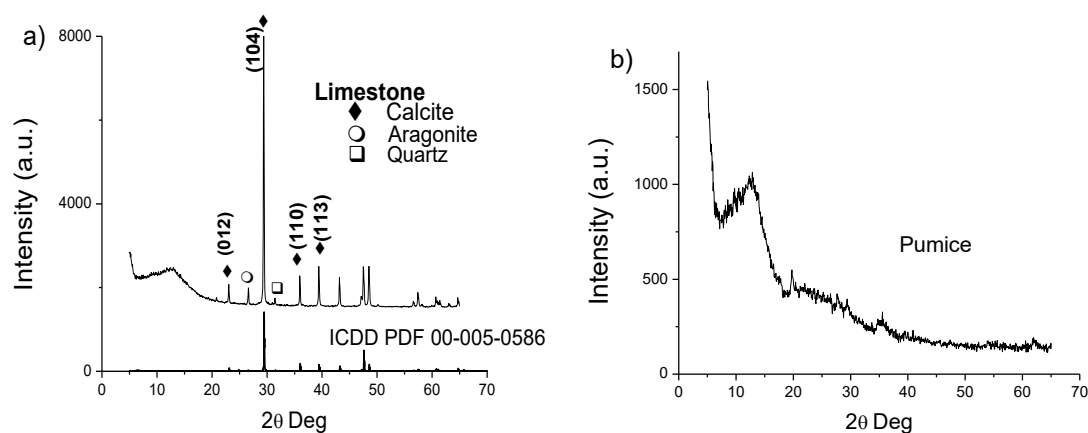
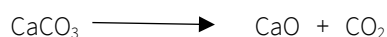


Figure 1. XRD patterns of a) Limestone and b) Pumice.

Table 3. Expansion percentage of formulations at 800°C- 20 min.

Sample	Expansion (%)
5-5-90	50
5-10-85	10
5-15-80	5

To verify the formulation behavior and sintering performance, some TGA-DSC analyses were performed to the 90-5-5 sample (Fig. 2). The thermogram showed a loss of weight in the temperature range of 580-700°C. In this region, CO₂ is produced because of the thermal decomposition of calcium carbonate as is showed in the chemical reaction:



The obtained weight for this decomposition reaction was 2.1% (expressed as released CO₂). Based on this amount, the stoichiometric ratio of calcium carbonate was calculated; this value is equivalent to a 4.8% content shown as pure CaCO₃ in the sample. The complement (0.2%) regarding the initial formulation as limestone (5%) was identified as quartz by XRD. Based on DSC analyses, an endothermic type signal was observed, corroborating the sample decarbonation. Even though the graph shows that the foaming action of CaCO₃ starts at 580°C, it must be considered that the released CO₂ has crossed through the compacted sample; thus, sintering temperature was markedly increased.

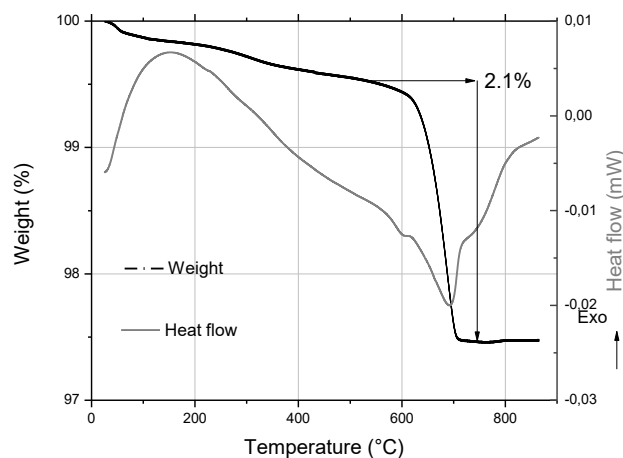


Figure 2. TGA-DSC thermal curves of 90-5-5 samples.

Once the optimal formulation was obtained, some sintered samples were prepared using sintering temperatures of 700, 750, 800 and 850°C with a furnace and a holding time of 20 minutes. The SEM micrographs of Fig. 3 showed an increased porous generation as a temperature rise in the 5-5-90 sample. It is noticeable that at 700°C, no pores are formed yet, the 750°C sample showed an incipient porosity generation in the form of small pores. At 800 and 850°C, pores increased their sizes because small pores communicate with each other forming larger pores. In the graphs of Fig. 4b the measurements of bulk density are displayed, it is observed that the 700°C sample had a value of 1.7 g/cm³, this indicates that carbonate decomposition does not happen yet and is corroborated in Fig. 4a where it is noticed that the sample had no apparent expansion. The minimum reached density values were 0.42 and 0.44 g/cm³ for temperatures of 850 and 800°C, respectively. The nominal difference between these two samples was minimal, so it was decided to use the lower sintering temperature (800°C) to evaluate the effect of holding time in the furnace to sintered samples. A critical disadvantage of sintering at a higher temperature (850°C) is the economic aspect translated as energy and investment-related costs. Besides, at a higher temperature, the glass component flows quickly, causing the sample to lose symmetry when it expands, as can be seen in the image of Fig. 4a, where the specimen looked heavily deformed. The graph of Fig. 4c shows the porosity level of sintered samples expressed as a percentage. The highest porosity was 83%, reached at 800 and 850°C.

As was mentioned above, the 5-5-90 sample sintered to 800°C was subjected to different holding times in the furnace. In Fig. 5a, it can be observed that a minimum value of bulk density was reached after 20 minutes of heating, obtaining the highest porosity percentage (81%). In the graphs, there is no significant difference in bulk density and porosity under different sintering times. It was observed that after 20 min, the samples begin to densify; this is probably due to glass creep that clogged the pores and deformed the sample simultaneously. The thermal conductivity is shown in Fig. 5b, as can be seen, these results have a direct relation to density, obtaining the lowest values 0.090 and 0.091 W/m K in samples heated at 850 and 800°C, respectively. These values are acceptable when they are compared with commercial polymer-based insulators such as expanded polystyrene and polyurethane, whose approximate values are 0.040 W/m K. As was mentioned earlier, these insulators have the critical disadvantages of not being able to use them in interior spaces because they are highly flammable and present higher involved costs.

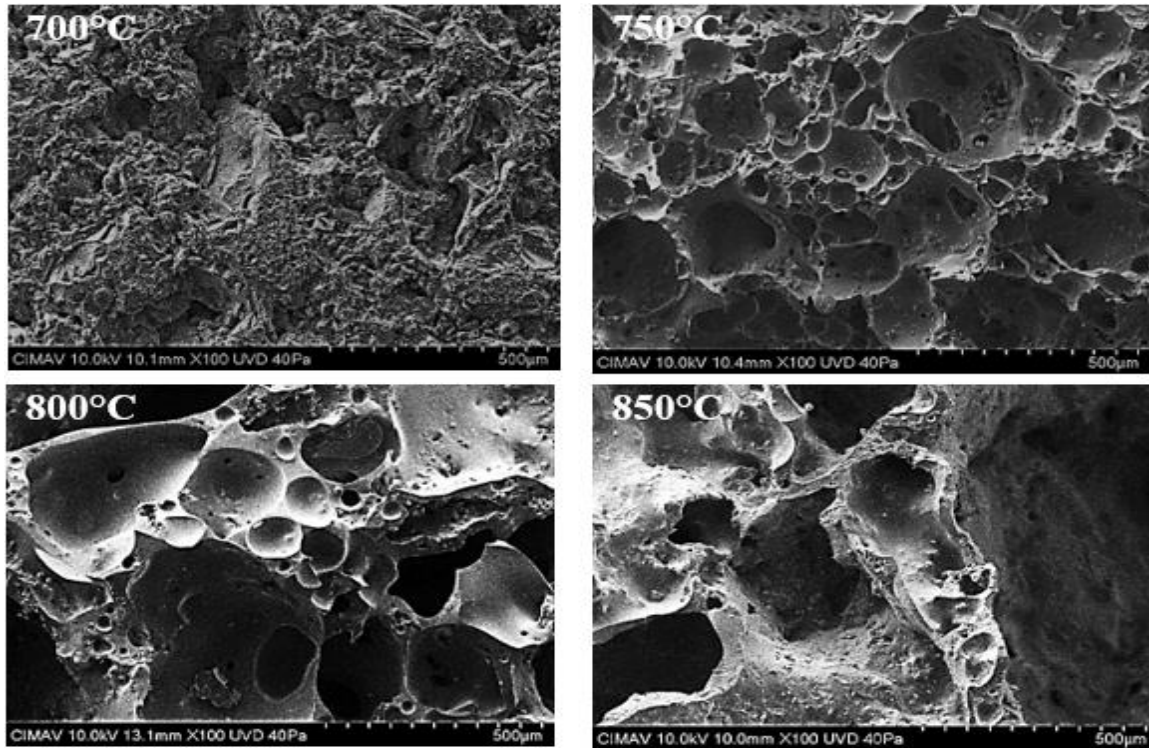


Figure 3. SEM micrographs of samples obtained at different sintering temperatures.

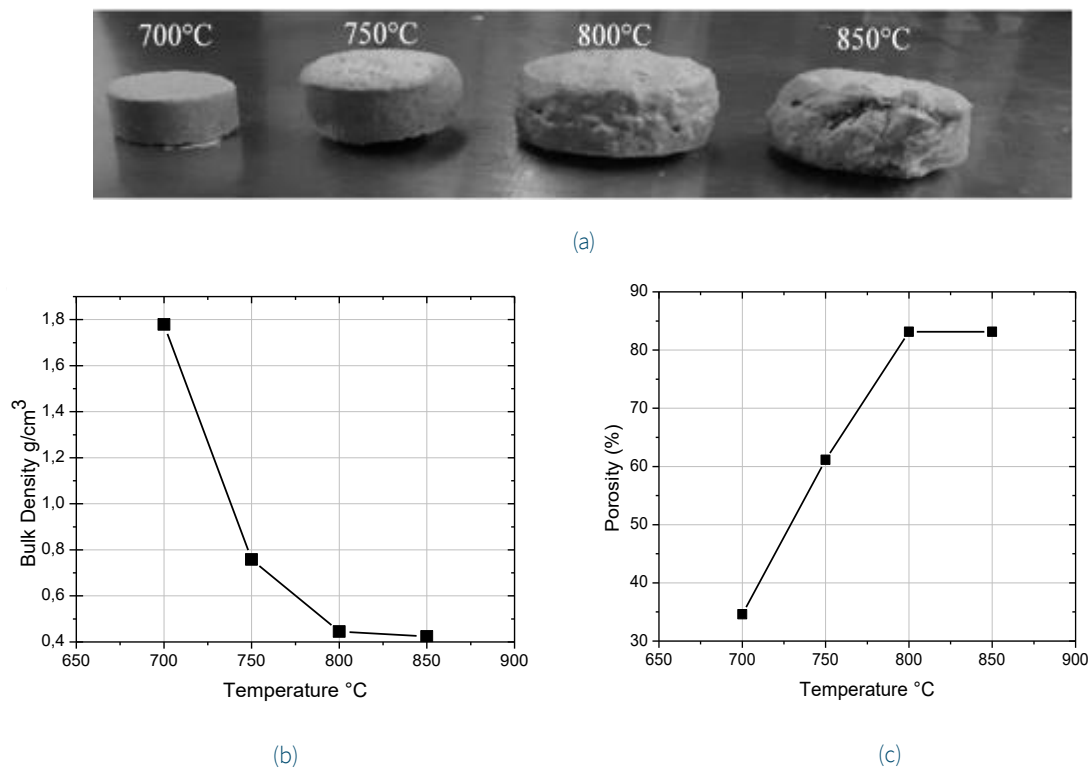


Figure 4. a) general images, b) bulk density and c) porosity of sintered 5-5-90 samples obtained as a function of temperature.

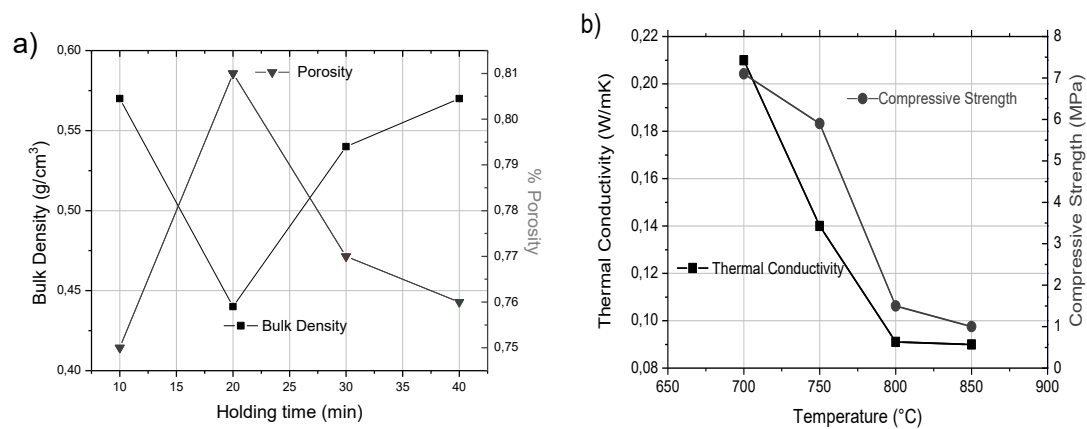


Figure 5. a) Bulk density and porosity of 5-5-90 the sample at 800°C under different sintering times, b) thermal conductivity and compressive strength as a function of sintering temperature.

Some compressive resistant tests were performed on sintered samples and their results are shown in Fig. 5b. Similarly, this property had a direct relationship with thermal conductivity. Both properties have great importance for the use of this material as an insulating barrier since this material usually goes as an outer layer and it must resist accidental impacts. Sintered samples at 800 and 850°C have a resistance of approximately 1 MPa; this value is similar to the results reported by Attila, Güden, and Taşdemirci (2013) and Baino and Ferraris (2019), which synthesized similar foams from vitreous materials. The pore size distribution of the 5-5-90 sample was determined and showed in Fig. 6, 300 measurements were made and the results were classified into 17 pore size intervals. The range of 0.55 to 0.63 mm was the most frequent, with a value of 59%. The total pore size range was 0.14 to 1.53 mm. A summary of the most important parameters for applications, such as an insulating coating of the 5-5-90 sample sintered at 800°C is presented in Table 4.

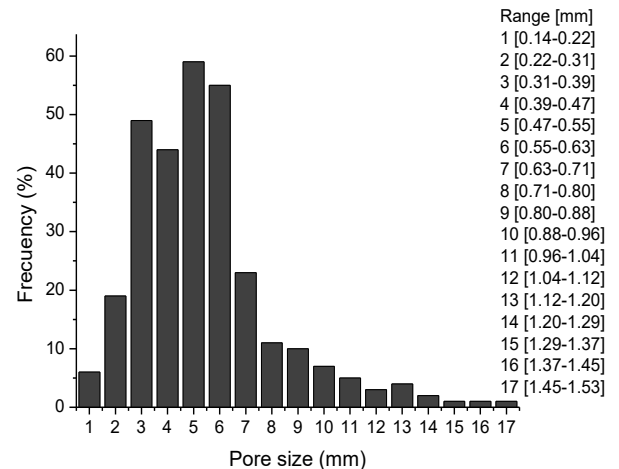


Figure 6. Histogram of the pore size distribution of 5-5-90 samples.

4. Conclusions

In this work, it was possible to synthesize ceramic foams prepared from a vitrocement mixture, using low-cost and a straightforward process. As precursors, some local industrial residues were used; this has a distinct advantage as low transport and inherent costs related to the acquisition of raw materials. The optimum sintering time was determined to be 20 minutes in comparison to longer residence times. The sintered ceramic foam with a 5-5-90 formulation at 800°C presented the best properties with 0.44 g/cm³ (bulk density) and a thermal conductivity coefficient of 0.096 W/m K; these values indicated that it is feasible to synthesize these foams for applications in the construction industry as available thermal insulators.

Table 4. Summary chart with thermal and mechanical characteristics of 5-5-90 (800°C) sample.

Parameter	Units	Measurement
Bulk Density	g/cm ³	0.44
Porosity	%	81
Expansion	%	50
Thermal Conductivity	W/m K	0.096
Compressive Strength	MPa	1.5
Pore size	mm	0.5

Acknowledgments

The authors gratefully thank L. de La Torre and P. Castillo for his technical analysis. C. Leyva, K. Campos. and E. Lestarjette for their help by SEM and XRD data acquisition, and Nanotech Lab, CIMAV, Chihuahua, Mexico. For their valuable technical support during the experimental development of the present study.

References

- Attila, Y., Güden, M., & Taşdemirci, A. (2013). Foam glass processing using a polishing glass powder residue. *Ceramics International*, 39(5), 5869-5877. <https://doi.org/10.1016/j.ceramint.2012.12.104>
- Bai, J., Yang, X., Xu, S., Jing, W., & Yang, J. (2014). Preparation of foam glass from waste glass and fly ash. *Materials Letters*, 136, 52-54. <https://doi.org/10.1016/j.matlet.2014.07.028>
- Baino, F., & Ferraris, M. (2019). Production and characterization of ceramic foams derived from vitrified bottom ashes. *Materials Letters*, 236, 281-284. <https://doi.org/10.1016/j.matlet.2018.10.122>
- Bento, A. C., Kubaski, E. T., Sequinel, T., Pianaro, S. A., Varela, J. A., & Tebcherani, S. M. (2013). Glass foam of macroporosity using glass waste and sodium hydroxide as the foaming agent. *Ceramics International*, 39(3), 2423-2430. <https://doi.org/10.1016/j.ceramint.2012.09.002>
- Bernardo, E., Cedro, R., Florean, M., & Hreglich, S. (2007). Reutilization and stabilization of wastes by the production of glass foams. *Ceramics International*, 33(6), 963-968. <https://doi.org/10.1016/j.ceramint.2006.02.010>
- Chen, X., Lu, A., & Qu, G. (2013). Preparation and characterization of foam ceramics from red mud and fly ash using sodium silicate as foaming agent. *Ceramics International*, 39(2), 1923-1929. <https://doi.org/10.1016/j.ceramint.2012.08.042>
- Correcher, V., Gomez-Ros, J. M., Dogan, T., García-Guinea, J., & Topaksu, M. (2017). Optical, spectral and thermal properties of natural pumice glass. *Radiation Physics and Chemistry*, 130, 69-75. <https://doi.org/10.1016/j.radphyschem.2016.08.002>
- Ding, L., Ning, W., Wang, Q., Shi, D., & Luo, L. (2015). Preparation and characterization of glass-ceramic foams from blast furnace slag and waste glass. *Materials Letters*, 141, 327-329. <https://doi.org/10.1016/j.matlet.2014.11.122>
- Guo, Y., Zhang, Y., Huang, H., Meng, K., Hu, K., Hu, P., & Meng, X. (2014). Novel glass ceramic foams materials based on red mud. *Ceramics International*, 40(5), 6677-6683. <https://doi.org/10.1016/j.ceramint.2013.11.128>
- Ji, R., Zhang, Z., He, Y., Liu, L., & Wang, X. (2015). Synthesis, characterization and modeling of new building insulation material using ceramic polishing waste residue. *Construction and Building Materials*, 85, 119-126. <https://doi.org/10.1016/j.conbuildmat.2015.03.089>
- Kato, T., Ohashi, K., Fuji, M., & Takahashi, M. (2008). Water absorption and retention of porous ceramics fabricated by waste resources. *Journal of the Ceramic Society of Japan*, 116(1350), 212-215. <https://doi.org/10.2109/jcersj2.116.212>
- Liu, T., Li, X., Guan, L., Liu, P., Wu, T., Li, Z., & Lu, A. (2016). Low-cost and environment-friendly ceramic foams made from lead-zinc mine tailings and red mud: foaming mechanism, physical, mechanical and chemical properties. *Ceramics International*, 42(1), 1733-1739. <https://doi.org/10.1016/j.ceramint.2015.09.131>
- Meir, I. A., & Roaf, S. C. (2006). Confort térmico-masa térmico: vivienda en climas cálido-secos. *Estudios del desierto*. ISBN 970-701-734-1.
- Ozel, M. (2011). Effect of wall orientation on the optimum insulation thickness by using a dynamic method. *Applied Energy*, 88(7), 2429-2435. <https://doi.org/10.1016/j.apenergy.2011.01.049>
- Presas Mata, M. (2008). Comportamiento mecánico de materiales celulares de carburo de silicio (*Doctoral dissertation, Caminos*). <http://oa.upm.es/1264/>. <https://doi.org/10.1016/j.apenergy.2011.01.049>
- Sousa, A., Amorim, K., Medeiros, E., Mélo, T., & Rabello, M. (2006). The combined effect of photodegradation and stress cracking in polystyrene. *Polymer Degradation and Stability*, 91(7), 1504-1512. <https://doi.org/10.1016/j.polymdegradstab.2005.10.002>
- Vancea, C., & Lazău, I. (2014). Glass foam from window panes and bottle glass wastes. *Central European Journal of Chemistry*, 12(7), 804-811. <https://doi.org/10.2478/s11532-014-0510-x>
- Wu, J. P., Boccaccini, A. R., Lee, P. D., Kershaw, M. J., & Rawlings, R. D. (2006). Glass ceramic foams from coal ash and waste glass: production and characterization. *Advances in Applied Ceramics*, 105(1), 32-39. <https://doi.org/10.1179/174367606X81632>